energyequipsys/ Vol 3/No2/Dec 2015/ 97-111

ENERGY EQUIPSYS

Energy Equipment and Systems

http://energyequipsys.ut.ac.ir
www.energyeuquipsys.com

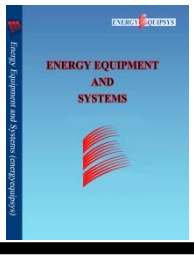

Numerical simulation of Al_2O_3–water nanofluid mixed convection in an inclined annulus

Authors

Hadi Imani [a]
Ali Cheraqi [b]
Ali Jafarian [a*]
Mohammad Mahdi Heyhat [a]

[a] Faculty of Mechanical Engineering, Tarbiat Modares University, Iran
P.O. Box 14115-143 Tehran, Iran

[b] Faculty of Aerospace Engineering, KNTU, P .O. Box 16765-3381 Tehran, Iran

Article history:

Received : 2 September 2015
Accepted : 28 October 2015

ABSTRACT

Laminar mixed convection of Aluminium oxide (Al_2O_3)–water nanofluid flow in an inclined annulus using a single-phase approach was numerically studied. Constant heat flux boundary conditions were applied on the inner and outer walls. All the thermophysical properties of nanofluid, such as, viscosity, heat capacity, thermal conductivity, and thermal expansion coefficient, except density in the body force term were assumed to be constant. Based on Boussinesq's hypothesis, density was assumed to be a linear function of temperature. The nanofluid properties were calculated in terms of constant properties of nanoparticles and the base fluid. Using the finite volume method the continuity, momentum, and energy equations were numerically solved. Numerical simulations were conducted for the nanoparticle concentrations of 0, 2, and 5% and five different inclination angles including -30°, -15° ,0 , +15°, and+30°. Results showed that a variation in the inclination angle affected the Nusselt number on the inner wall more than the outer one. The Nusselt number in negative angles was higher than in the positive ones, so that at a volume fraction of 5%, the average Nusselt number at the inner wall decreased almost 2% when changing the angle from -30° to+30°. The local Friction factor in the positive angles was higher than in the negative ones.

Keywords: Inclined Annulus, Laminar, Mixed Convection, Nanofluid.

1. Introduction

To manage the growing demand from different developed industries, heat exchanger devices have to be smaller and have a higher performance. Low thermal conductivity of conventional heat transfer fluids such as water and oil is an important factor in optimizing the efficiency and compactness of various engineering equipment. There is an intensive stimulus to develop advanced heat transfer mediums, with especially higher thermal conductivity, to dominate this drawback. Suspending very fine solid particles that have high thermal conductivity in the fluid is a good way to improve the thermal conductivity of fluids. Improving the technology leads to making particles in nanometer dimensions and consequently a new generation of solid–liquid mixtures that are called nanofluids [1]. A nanofluid is a suspension of nanoparticles such as Aluminium oxide (Al_2O_3), Cupric oxide (CuO) in a base fluid such as water, ethylene glycol or oil. It has been found that the thermal conductivity of a nanofluid is significantly higher than that of the base fluid. Many researches in this field have been done to formulate the effective properties of a

*Corresponding author: Ali Jafarian
Address: Faculty of Mechanical Engineering, Tarbiat Modares University, Iran; P.O. Box 14115-143 Tehran, Iran
E-mail address: jafarian@modares.ac.ir

nanofluid such as thermal conductivity [2, 3, 4] and dynamic viscosity [5,6].

Two-phase or single-phase approaches can be applied for simulating convective heat transfer with a nanofluid. The single-phase approach is simpler and requires less computational time. It assumes that the base fluid and the nanoparticles are in thermal and hydrodynamic equilibrium. This approach has been used in many theoretical studies of convective heat transfer with nanofluids [7-13].

Buoyancy-induced convection in annular tubes between differentially heated, horizontal, concentric cylinders have a substantial role to play in a number of engineering applications, such as, heat exchangers, solar collectors, thermal storage systems, and cooling of electronic components. One of the most common applications of an annular tube is the tube in a tube heat exchanger where a medium fluid that flows between two cylinders transfers the heat between hot and cold fluids inside the inner tube and outside the outer tube. Investigation of the heat transfer in annular tubes is essential. Abu-Nada [14] studied the single-phase Al_2O_3–-water nanofluid flow in an annular pipe; He used different viscosity and thermal conductivity models to evaluate heat transfer enhancement in an annular pipe. He [15] also studied various nanofluids consisting of water as a base fluid and different solid nanoparticles including Copper (Cu), Silver (Ag), Al_2O_3, and Titanium dioxide (TiO_2) in a horizontal annulus. Izadi et al. [16] investigated laminar forced convection of a nanofluid consisting of Al_2O_3 and water, numerically, in a two-dimensional annulus with a single-phase approach. Ben Mansour et al. [17] experimentally studied the mixed convection of an Al_2O_3–-water nanofluid inside an inclined tube submitted to a uniform wall heat flux at its outer surface. Mokhtari et al. [18] studied the heat transfer enhancement of a mixed convection laminar Al2O3–-water nanofluid flow in an annulus with constant heat flux boundary conditions.

In this study, by employing the single-phase approach, the nanofluid flow in an inclined annular pipe is considered. The objective is to study the impact of the inclination angle, the nanoparticle's volume fraction (Φ), and the buoyancy force in the laminar mixed convection of nanofluid flow in an inclined annular pipe. To reach this aim, laminar mixed convection in Al_2O_3–water nanofluid flow in the inclined annulus is investigated. Effects of the nanoparticle's volume fraction (Φ), different ratios of the heat fluxes from the outer wall to the inner wall, and five inclination angles including -30°,-15° ,0 , +15° and +30°on the axial velocity, secondary flow patterns, friction factor. and Nusselt number profiles are presented and discussed.

Nomenclature

C_f	Friction factor
c_p	Heat capacity, $[J/k.K]$
D	Diameter, $[m]$
D_h	Hydraulic diameter, $[m]$
g	gravitational acceleration, $[m/s^2]$
Gr	Grashof number
h	Heat transfer coefficient, $[W/m^2.K]$
k	Thermal conductivity, $[W/m.K]$
P	Pressure, $[pa]$
q''	Heat flux, $[W/m^2]$
Re	Reynolds number
Ri	Richardson number, (Gr/Re^2)
T	Temperature, $[K]$
U	Velocity vector, $[m/s]$
x, y, z	Cartesian coordinate directions

Greek symbols

α	Inclination angle
β	Thermal expansion coefficient, $[1/K]$
ϕ	Nanoparticle volume fraction
μ	Viscosity, $[kg/m.s]$
ρ	Density, $[kg/m^3]$
τ	Shear stress

Subscripts

b	bulk
f	Fluid
m	Mixture
p	Particle
w	Wall

2.Physical Model

The geometry of the considered problem is schematically depicted in Fig.1. The computation domain is composed of an inclined straight annulus pipe of length L, with inner and outer diameters of D_i and D_o respectively, whereas, the gravitational force is exerted vertically. The global coordinate system is on the pipe and the gravitational force has two angles with y and z directions based on the inclination angle of the pipe, which varies from -30° to +30°. The channel length (L) is supposed to be 200 times the hydraulic diameter (D_h), to insure that the fully developed condition is reached at the outlet. The nanofluid flow is laminar, steady state, and incompressible, while the dissipation and pressure work are neglected. All the properties of the nanofluid are assumed to be constant, except for the density in the body force, which varies linearly with the temperature (Boussinesq's hypothesis).

3.Mathematical Modeling

Analysis of the fluid flow and heat transfer of the nanofluid into an annulus is a very complicated process. ANSYS CFX-11.0 was employed to simulate the problem. The discrete system of linearized equations has been solved using a Multi-grid accelerated Incomplete Lower–Upper (ILU) factorization technique. The Multi-grid process performs on a fine mesh in early iterations and onprogressively coarser virtual ones in later iterations. Although with this method, a single iteration is slower than that of the classical decoupled SIMPLE approach; therefore, the number of iterations necessary for a full convergence is generally in the order of 10^2 against typical values of 10^3 for decoupled algorithms. A structured grid system is composed of hexahedral elements, which is schematically depicted in Fig.2, and is used to discretize the computation domain. The total number of elements in the meshed body are 1,200,000, which are produced by selecting

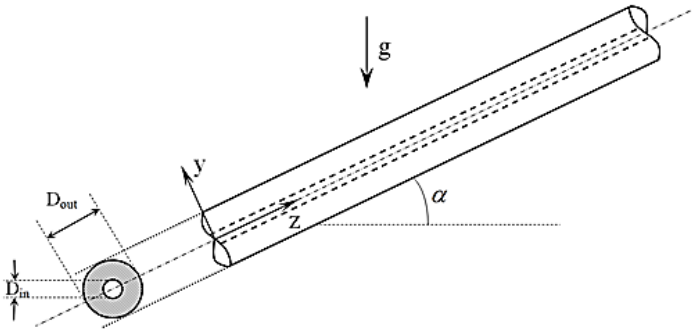

Fig. 1. Problem geometry and coordinate system

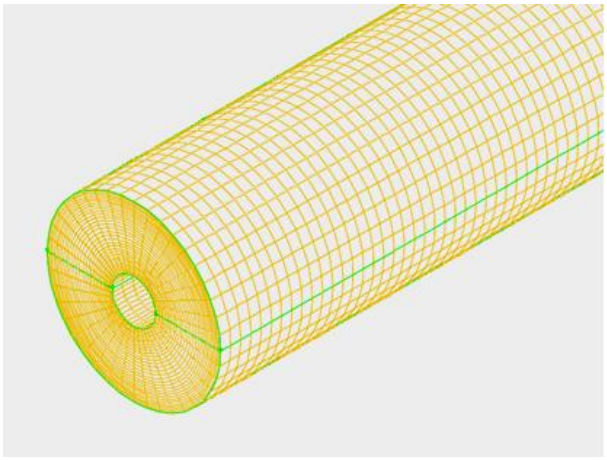

Fig. 2. Mesh used to perform the computations

the $1000\times40\times30$ grid for the present calculations in the axial (z), tangential (θ), and radial (r) directions, respectively.

3.1.Governing Equations

The governing equations, as follows, were solved, to simulate the fluid flow and heat transfer in the Cartesian coordinate system. The continuity, momentum, and heat transfer equations used in the present study are as follows:

$$\nabla.(\rho_m U_m)=0. \quad (1)$$

$$\nabla.(\rho_m U_m U_m)=-\nabla p+\nabla.(\mu_m \nabla U_m) - \rho_m \beta_m g(T-T_i). \quad (2)$$

$$\nabla.(\rho_m c_{pm} U_m T)=\nabla.(k_m \nabla T). \quad (3)$$

The well-known correlations for calculating the thermophysical properties of the nanofluid are often cited by a number of researchers and are expressed in the following.

3.2.Nanofluid Properties

The single-phase approach was employed in the simulation by assuming that the properties of the nanofluid were constant. The properties of water and the Al_2O_3 nanoparticles, to calculate the mixture properties, are given in Table 1.

3.2.1.Thermal Conductivty

The effective thermal conductivity of a nanofluid dating back to the classical study of Maxwell [19] is given by:

$$k_m=k_f\left[\frac{k_p+2k_f-2\phi(k_f-k_p)}{k_p+2k_f+\phi(k_f-k_p)}\right]. \quad (4)$$

Based on Maxwell's expression, the effective thermal conductivity of a nanofluid is calculated in terms of thermal conductivity of the spherical particles, the base fluid, and the volume fraction of the solid particles.

3.2.2.Density and Specific Heat

Calculation of the effective heat capacity and effective density of the nanofluid is very easy. It can be based on the physical principle of the mixture rule. These results have very good accordance with the experimental data. The density and the heat capacity based on Pak et al.[20] and Xuan et al.[21] are supposed to be in the following forms:

$$\rho_m=(1-\phi)\rho_f+\phi\rho_p. \quad (5)$$

$$c_{p,m}=\frac{(1-\phi)(\rho c_p)_f+\phi(\rho c_p)_p}{(1-\phi)\rho_f+\phi\rho_p}. \quad (6)$$

3.2.3.Viscosity

The viscosity is calculated using the Einstein equation [22], which is applicable to spherical particles in volume fractions of less than 5.0% and is defined as follows:

$$\mu_m=(1+2.5\phi)\mu_f. \quad (7)$$

3.2.4.Thermal Expansion Coefficient

Applying the expression by Khanafer et al.

Table 1. Thermophysical properties of nanoparticles and base fluid at 22°C

Properties	Water	Nanoparticle (Al_2O_3)
Density $\rho(kg/m^3)$	998.2	3720
Heat capacity $c_p(J/kg\ K)$	4182	880
Thermal conductivity $k(W/mK)$	0.6	35
Thermal expansion $\beta(1/K)$	0.0002374	0.0000082
Particle diameter (nm)	--	28

[23] the thermal expansion coefficient is calculated as follows:

$$\beta_m = \left[\frac{1}{1+\frac{(1-\phi)\rho_f}{\phi\rho_p}\frac{\beta_p}{\beta_f}} + \frac{1}{1+\frac{\phi\rho_p}{(1-\phi)\rho_f}} \right] \beta_f . \quad (8)$$

The properties of the nanofluid in Eqs. (4-8) are evaluated from water and nanoparticles at the mean bulk temperature.

3.3.Boundary Conditions

These set of governing-coupled non-linear differential equations are solved subject to the following boundary conditions:

- inlet ($z = 0$):

$U_{m,z} = U_{in}$, $U_{m,y} = U_{m,x} = 0$ & $T = T_i$.

- Internal wall: No slip boundary condition and constant heat flux.
- External wall: No slip boundary condition and constant heat flux.
- Outlet ($z = L$): Zero pressure condition.

In this study, the Friction coefficients at the inner and outer walls are calculated by:

$$C_{f,i} = \frac{\tau_{w,i}}{\frac{1}{2}\rho_m U_{in}^2}$$

and

$$C_{f,o} = \frac{\tau_{w,o}}{\frac{1}{2}\rho_m U_{in}^2} . \quad (9)$$

where τ_w is defined on the inner and outer walls.

The local Nusselt number (Nu) is calculated based on the inner and outer walls as follows:

$$Nu_i = \frac{h_i D_h}{k_m}$$

and

$$Nu_o = \frac{h_o D_h}{k_m} . \quad (10)$$

where

$$h_i = \frac{q''_{w,i}}{(T_{w,i} - T_b)}$$

and

$$h_o = \frac{q''_{w,o}}{(T_{w,o} - T_b)} . \quad (11)$$

The Reynolds and Grashof numbers are defined as follows:

$$\mathrm{Re} = \frac{\rho_m u_i D_h}{\mu_m}$$

and

$$Gr = \frac{g\beta_m q''_{net} D_h^4}{k_m \nu_m^2} \quad (12)$$

The Net heat flux is defined as follows:

$$q''_{net} = q''_{w,in} + q''_{w,out} \quad (13)$$

4.Results and Discussion

To demonstrate the validity and accuracy of the problem assumption and the numerical analysis for forced convection, the bulk temperature profile in a straight circular pipe ($D_i/D_o = 0$) was compared with the experimental results of Ben Mansour et al. [17] at $\mathrm{Re} = 620$ and $Gr = 4.5\times10^4$. Therefore, the Richardson number is quite low ($Ri \approx 0.1$) and these conditions correspond to a forced convection flow. Figure 3 shows that there is a good accordance between the experimental and numerical results.

For a mixed convection case, the numerical results of the convective heat transfer convection coefficient were compared with the values obtained from the experimental study of Ben Mansour et al. [17] at $\mathrm{Re} = 360$, $Gr = 7.3\times10^4$, and ($D_i/D_o = 0$) which the Richardson number is nearly one. As illustrated in Fig.4, there is good agreement between the numerical results of the Nusselt number and the experimental values.

Also the fully developed values of Nusselt numbers at the inner and outer walls were compared with the available numerical

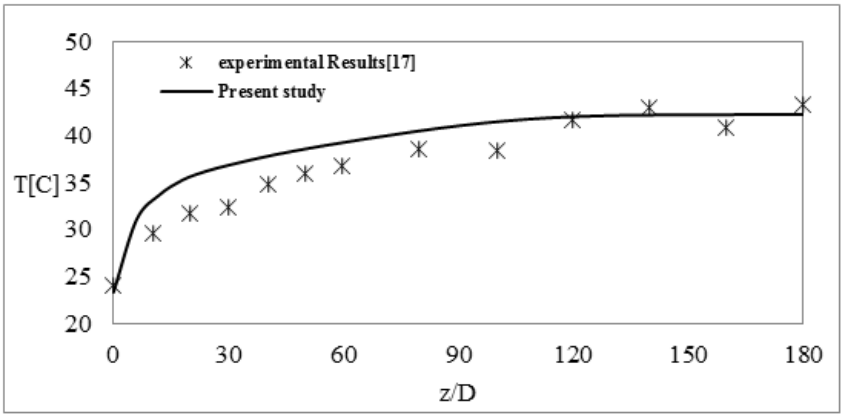

Fig. 3. Axial development of bulk temperature for forced convection

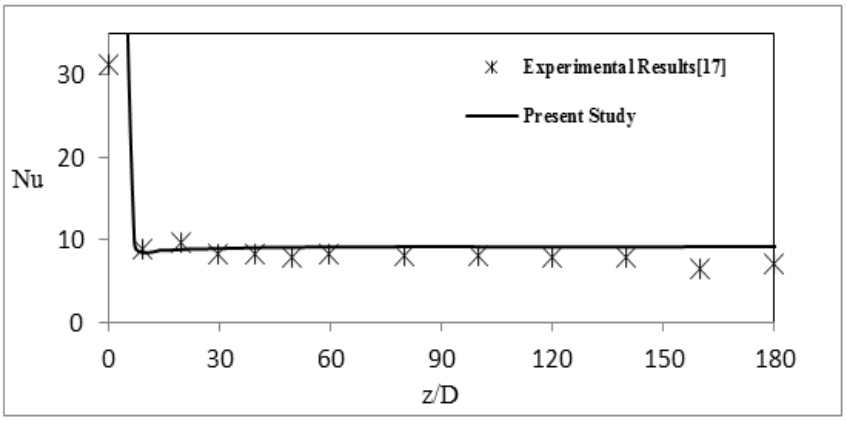

Fig. 4. Axial development of the Nusselt number for mixed convection

solutions for a mixed convection flow, in an annulus $(D_i/D_o = 0.25)$ carried out by Mokhtari et al. [18] at $\mathrm{Re} = 600$, $Gr = 3\times10^5$, $q_i/q_o = 0.5\,\&1$, and $\phi = 0.02$. As shown in Figs. 5 and 6, a good agreement exists between the simulated results and the reported numerical ones.

With the above comparisons the present numerical method is reliable, as it can predict the mixed convection nanofluid flow in an annulus.

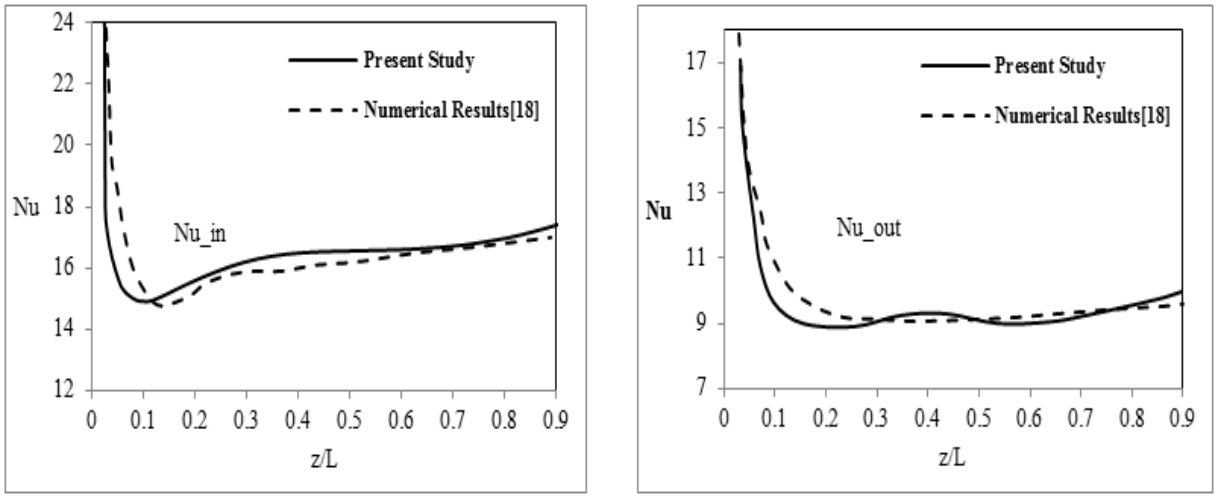

Fig. 5. Nusselt number at the inner and outer walls ($\mathrm{Re} = 600$, $Gr = 3\times10^5$, $q_i/q_o = 0.5$, and $\phi = 0.02$)

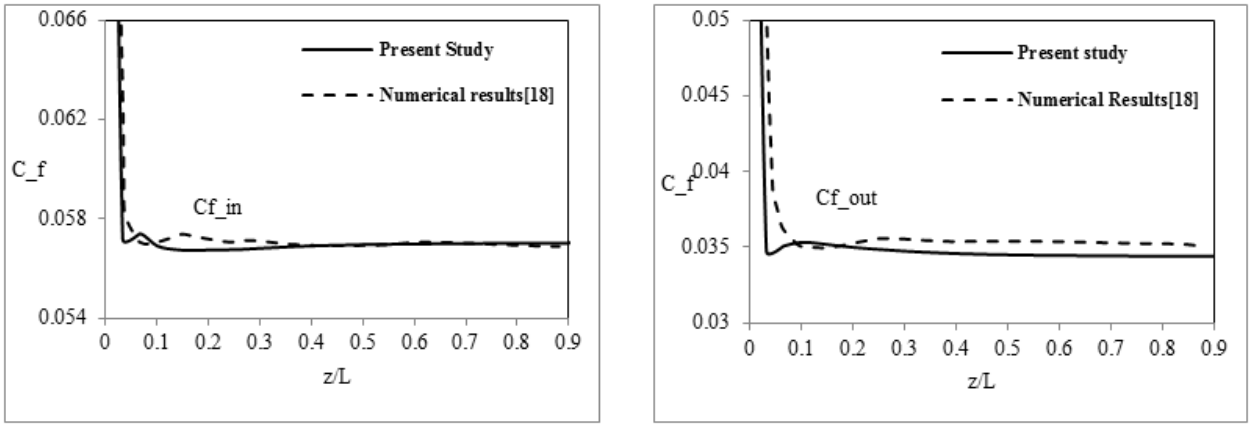

Fig. 6. Friction factor at the inner and outer walls ($\mathrm{Re}=600$, $Gr=3\times10^5$, $q_i/q_o=1$, and $\phi=0.02$)

In this study, effects of the inclination angle, solid nanoparticles volume fraction (ϕ), and heat flux ratios at the inner and outer walls on the hydrodynamical and thermal behaviors of the nanofluid flow in the annulus are presented and discussed. Numerical simulations are done in the five inclination angles, with different values of the nanoparticle volume fractions (0, 2 and 5%).The annulus aspect ratio (r_o/r_i) is assumed to be 4 and the nanoparticle's shape and diameter are assumed to be spherical and 28 nm, respectively. Also all the simulations have been done at $\mathrm{Re}=550$ and $Gr=3\times10^5$.

Figure 7 shows the effect of the heat flux ratio $(q''_{w,in}/q''_{w,out})$ on the streamlines, secondary flows, and non-dimensional temperatures at the end of the horizontal annulus at $\mathrm{Re}=550$ and $Gr=3\times10^5$. As shown in Fig.7, the more the heat flux ratio increases the more the vortices near the inner wall become stronger and consequently the vortices near the outer wall become weaker. In fact, with no heat flux on the inner wall $(q''_{w,in}/q''_{w,out}=0)$, there are only two vortices on the left and right sides of the annulus. Considering a heat flux on the inner wall, two vortices appear near that wall and they greaten

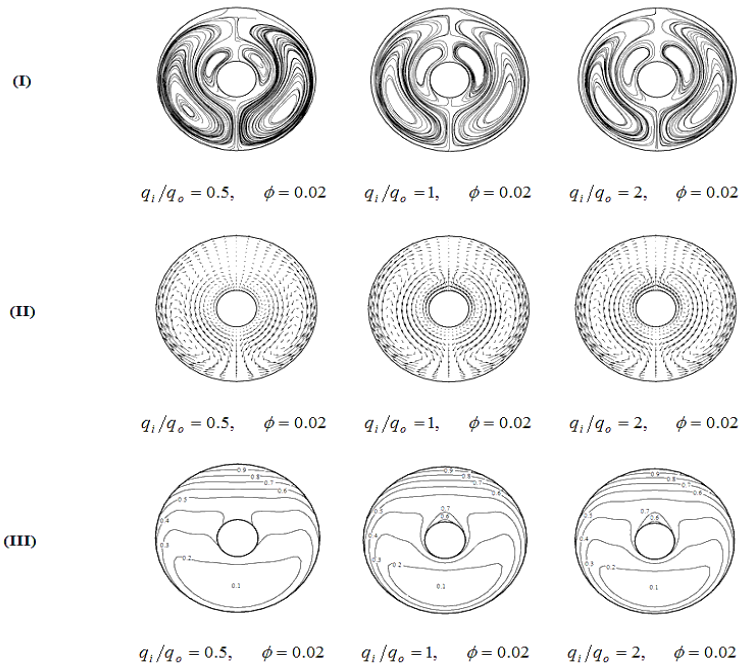

Fig. 7. Effects of the heat flux ratio ($q''_{w,in}/q''_{w,out}$) on the (I) Streamlines, (II) Secondary flows, and (III) contour of non-dimensional temperature

when the inner wall heat flux increases; this is because of the decrease in density of the nanofluid as a result of the inner wall heat flux.

The maximum temperature appears at the top of the annulus. Reversely, the maximum velocity appears at the bottom of the annulus. Also increasing the heat flux ratio, the isothermal lines bowed toward the inside of the annulus.

Effects of different inclination angles, varying from - 30° to 30° on the secondary flows, streamlines, and non-dimensional temperatures are depicted in Fig. 8. It is seen that the strength of the outer vortices reduces with the variation in the inclination angle

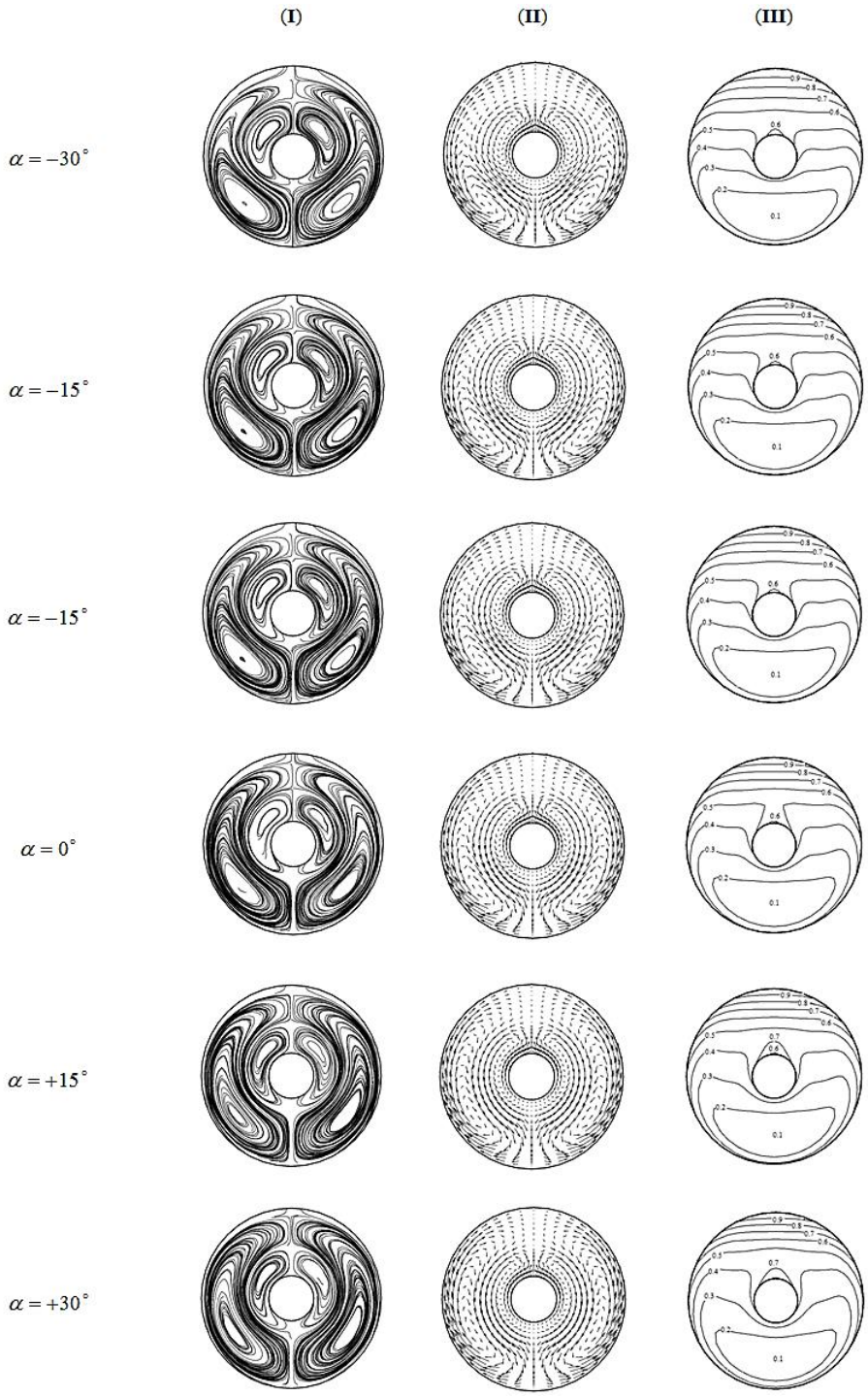

Fig. 8. Effects of variation of the inclination angle on the (**I**) Streamlines, (**II**) Secondary flows, and (**III**) contour of non-dimensional temperature at $\mathrm{Re} = 550$, $Gr = 3\times10^5$, and $\phi = 0.05$

from -30° to 30°; this is because of the direction of the gravity force, which is co-current with the flow in the negative angles and is in the opposite direction with the flow in the positive angles. Also the fluid temperature at the top half of the annulus becomes greater than that at the bottom half in positive angles rather than negative ones.

Increasing the solid particle concentration affects the temperature distribution and secondary flow as shown in Fig.9. The secondary flow strength increases as the solid nanoparticle concentration increases.

The effect of the inclination angles on the Nusselt numbers at the inner and outer walls are presented in Fig.10. On increasing the inclination angle, the Nusselt number at the inner wall reduces. This is because of the fact that the gravity force is co-current with the flow direction in the negative angles; so the fluid velocity at the end of annulus in positive angles is lower than in the negative ones.

Consequently, a higher amount of heat transfers into the fluid and the fluid temperature becomes higher than that in the lower angles; therefore, the Nusselt number becomes higher than that in the positive inclination angles.

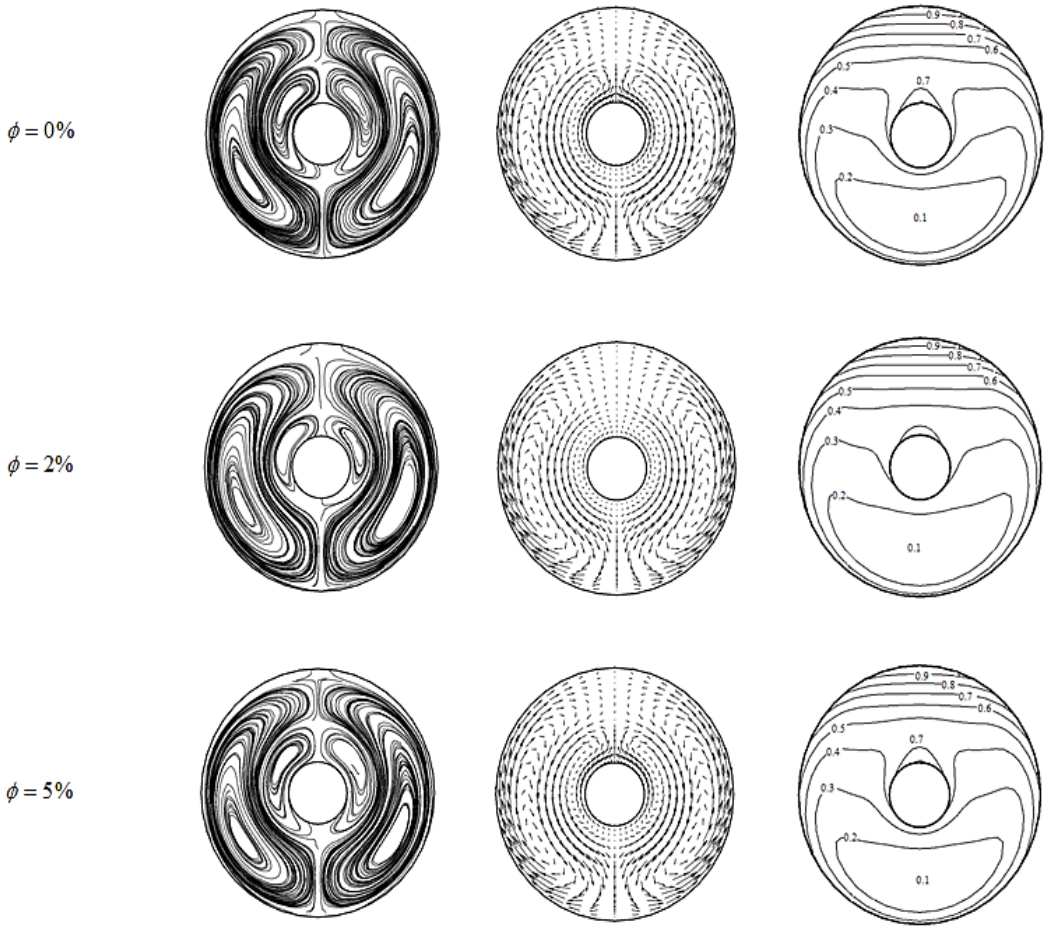

Fig. 9. Effect of particle concentration on (I) Streamlines, (II) Secondary flows and (III) contour of non-dimensional temperature at $\mathrm{Re} = 550$, $Gr = 3\times10^5$, and $\alpha = +30^\circ$

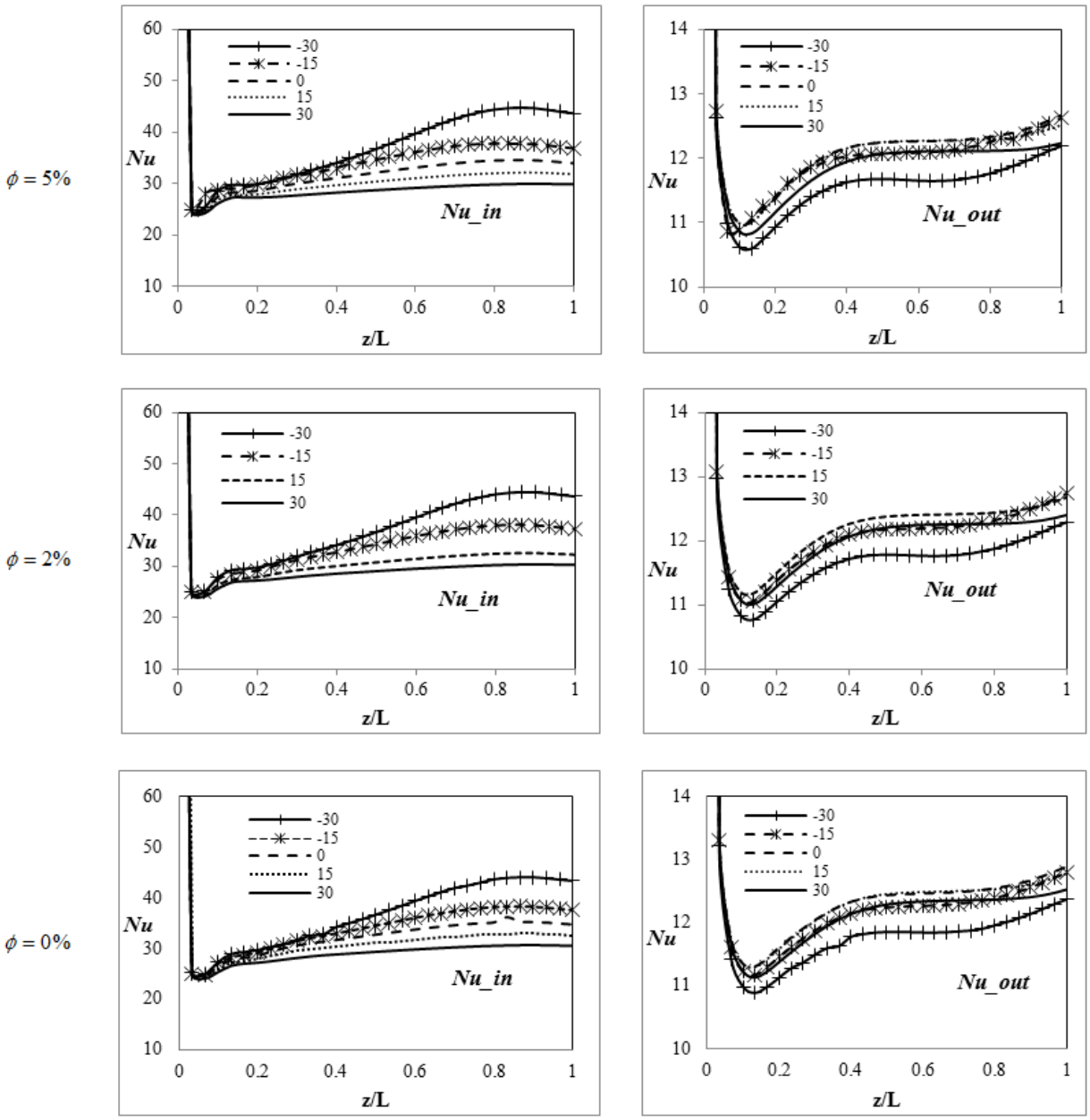

Fig. 10. Effect of the inclination angle on the Nusselt number at the inner and outer walls at different volume fractions

Figure 11 shows the average Nusselt number at the inner and outer walls for different nanoparticle concentrations and inclination angles. As shown, changing the inclination angle from -30° to +30°, causes the average Nusselt number at the inner wall to reduce dramatically, however, the average Nusselt number at the outer wall tends to increase in the negative angles and decrease in the positive angles.

Friction factor at the outer wall shows a reverse behavior when changing the inclination angle from -30° to +30° (Fig. 12). Indeed with an increase in the inclination angle the Friction factor at the outer wall increases. Also both the Nusselt number and local Friction factor at the inner wall are higher than those at the outer wall.

The Nusselt number at the outer wall in the horizontal case is higher than in other cases. At the beginning of the pipe, the Friction factor at the inner wall in the case of -30° is lower than in the other cases and at the second half of the pipe the Friction factor at the inner wall in the case -30° grows quickly and dominates the other cases.

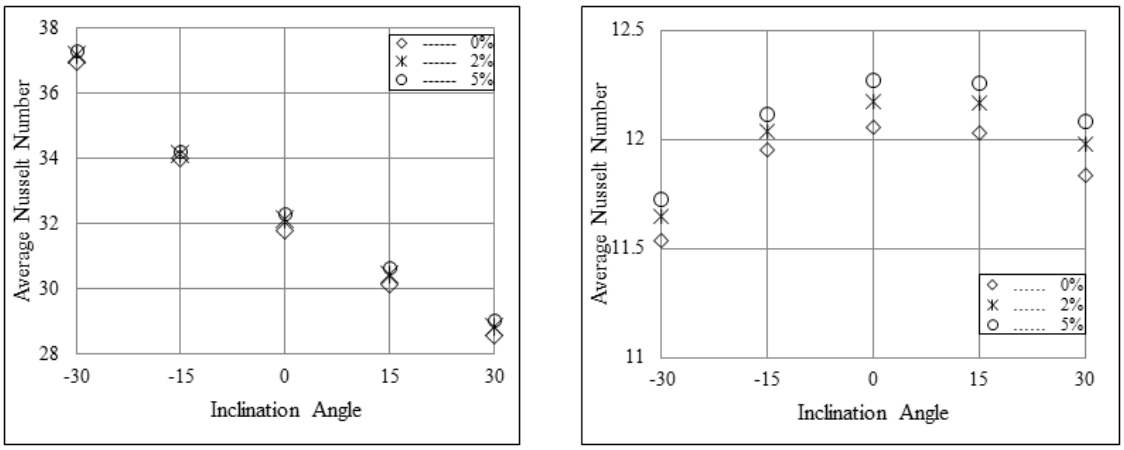

Fig. 11. Average Nusselt number at different inclination angles and nanoparticle concentrations (a) on the inner wall, (b) on the outer wall

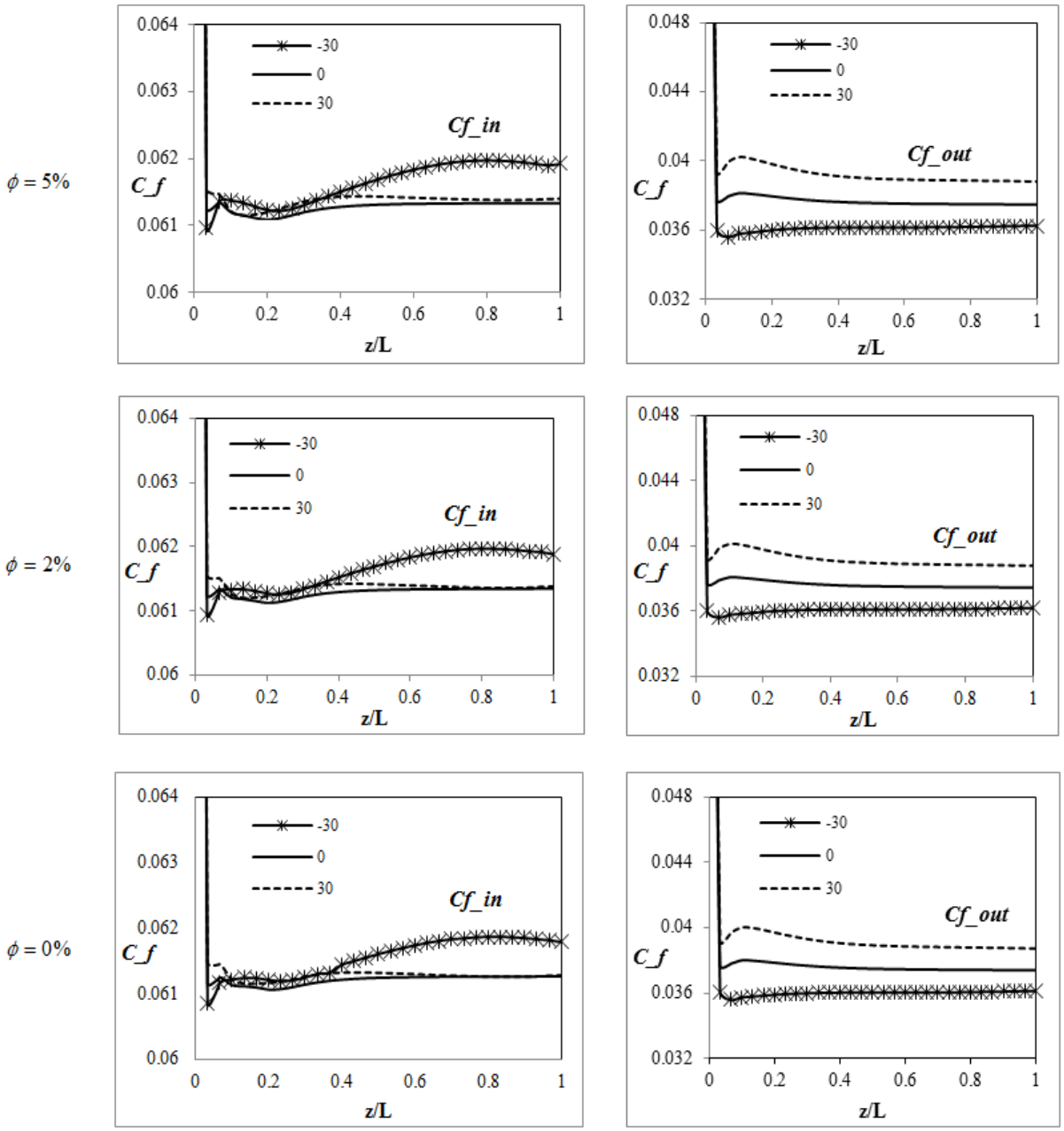

Fig. 12. Effect of inclination angle on the local Friction factor at the inner and outer walls at different volume fractions

Variation in the Nusselt number at the inner and outer walls at different particle concentrations is presented in Fig.13. It is clear that by increasing the particle concentration, the Nusselt number on the wall increases. A reverse behavior is shown in the variation of the local Friction factor at the inner and outer walls at different concentrations (Fig. 14).

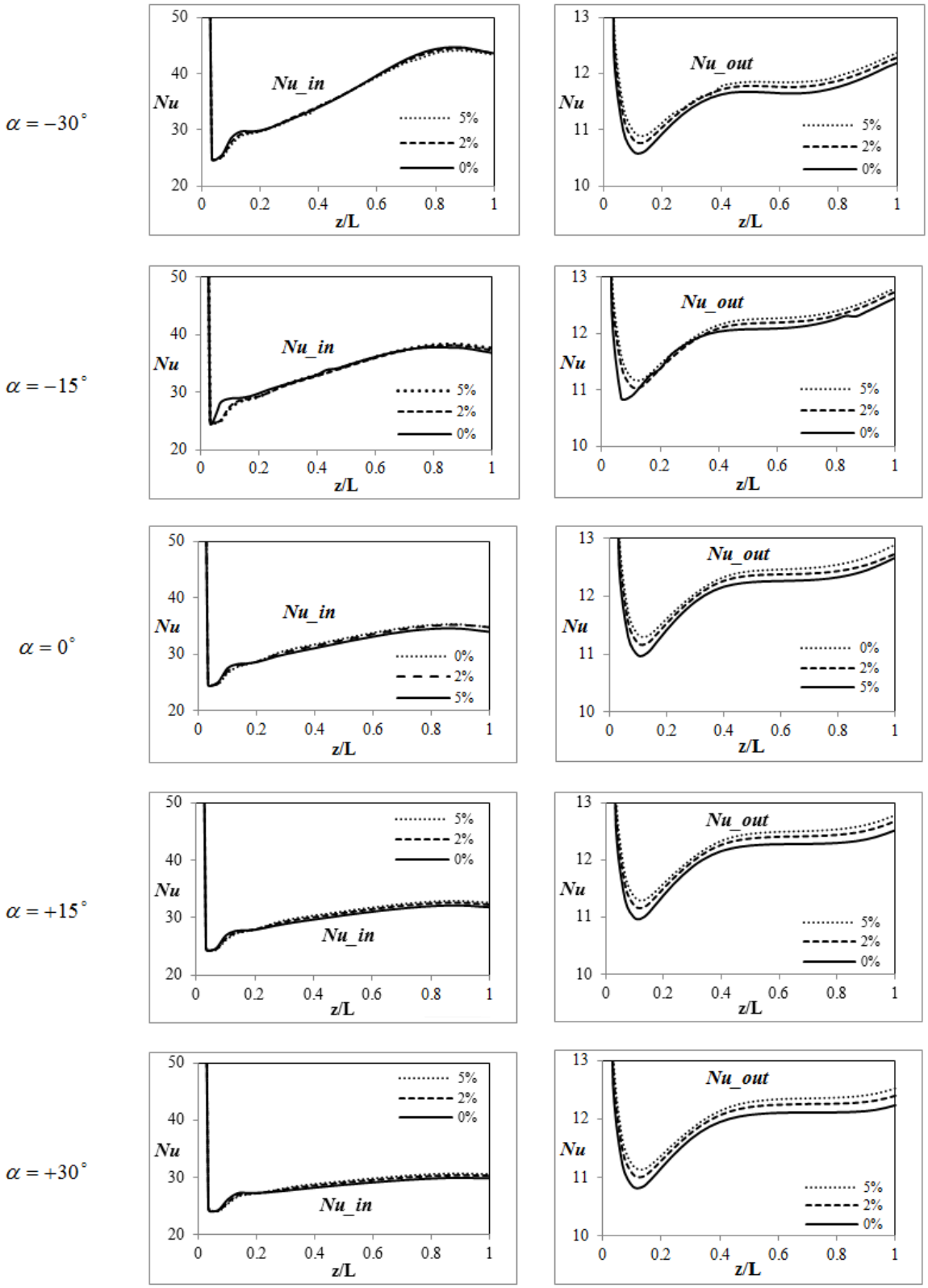

Fig. 13. Effect of volume fractions on the Nusselt number at the inner and outer walls at different inclination angles

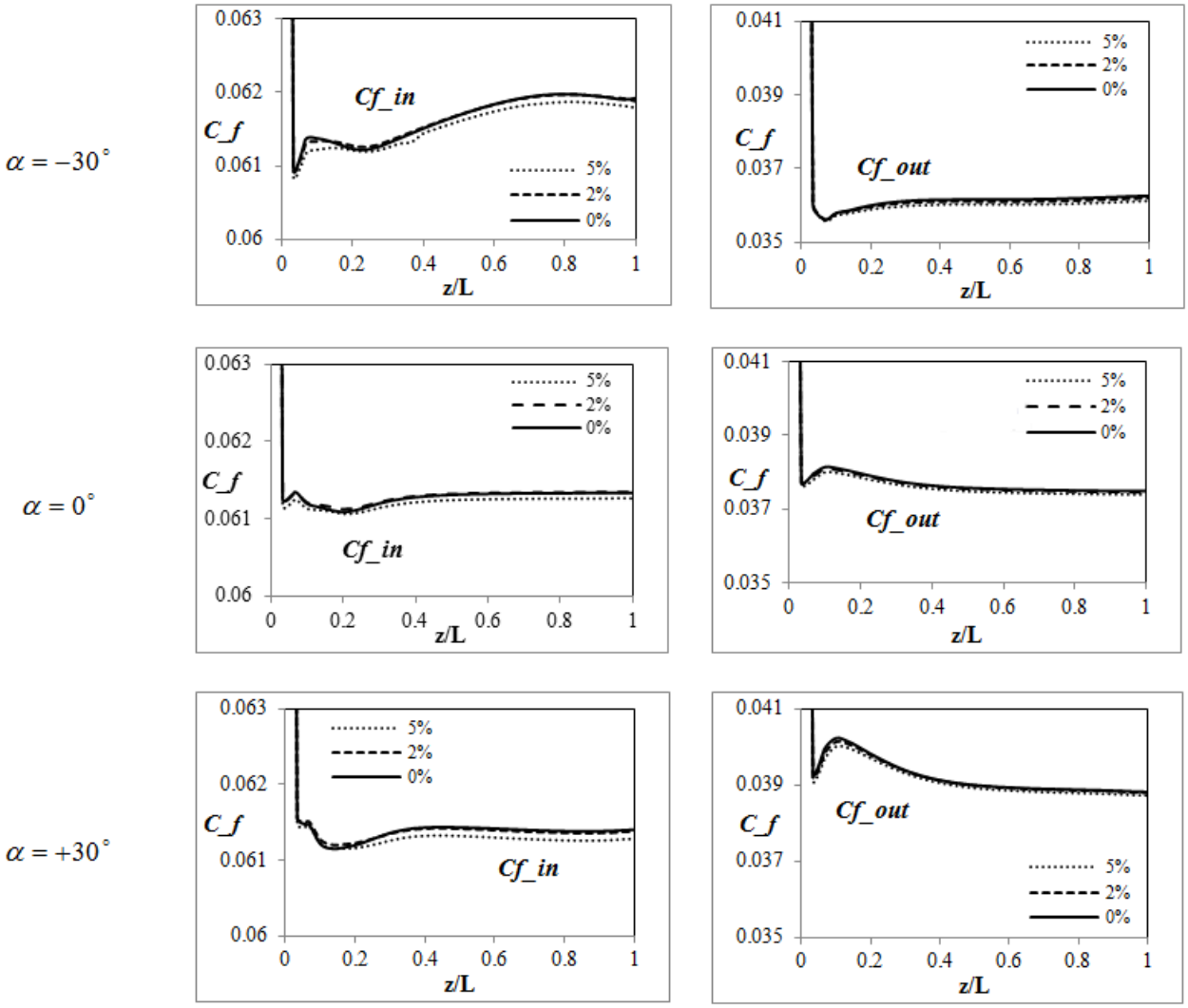

Fig. 14. Effect of volume fractions on the Friction factor at the inner and outer walls at different inclination angles

The amount of the local Friction factor and Nusselt number on the inner wall is greater than that on the outer wall in all cases. Also the vortices near the outer wall are stronger than those near the inner wall in all the cases. This is because of the fact that the amount of heat transfer from the outer wall is more than the heat transfer from the inner wall at equal heat fluxes. This is because of the vastness of the heat transfer surface of the outer wall in comparison to the inner wall.

5.Conclusion

Laminar mixed convection of the Al2O3–-water nanofluid flow inside an inclined annulus was numerically solved using the single-phase approach. Five different angles have been assumed for these simulations. All the thermophysical properties of nanofluids were calculated based on the nanoparticles and the base fluid constant properties. All the simulations were done at Re=550, $Gr = 3\times10^5$ and the heat flux ratio equal to one ($q''_{w,in}/q''_{w,out}=1$).

The results illustrated that deviating from the horizontal state, the Nusselt number and Friction factor were significantly changed. The Nusselt numbers in negative angles, in which the gravity force is co-current with the flow direction, were higher than in the other cases, hence at a volume fraction of Φ=5% the average Nusselt number at the inner wall in -30° was 37.3 and it reduced to 29 in+30°, and reversely, the Friction factor in those states was lower than in the other cases. The bulk temperature in the negative angles

was lower than in the positive ones and consequently the heat transfer coefficient in those cases was more than in the other cases. Similarly, the Friction factor in the negative angles was lower than in the other cases.

Temperature distribution uniformity in negative angles is more than in positive angles. With changing the inclination angle from negative to positive the hot fluid moves upward in the cross-section of the annulus, and therefore, the temperature difference between the upper and lower parts of the pipe increases. Also secondary flow strength in the negative angles is higher than in the positive angles.

References

[1] Choi S.U.S., Enhancing Thermal Conductivity of Fluid with Nanoparticles, Developments and Applications of Non-Newtonian Flow, ASME, FED 231/MD, 66 (1995) 99–105.

[2] Yu W., Xie H., Chen L., Li Y., Investigation of Thermal Conductivity and Viscosity of Ethylene Glycol Based ZnO Nanofluid, Thermochim. Acta, 491 (2009) 92–96.

[3] Zhang X., Gu H., Fujii M., Effective Thermal Conductivity and Thermal Diffusivity of Nanofluids Containing Spherical and Cylindrical Nanoparticles, Exp. Therm. Fluid Sci. 31 (2007) 593–599.

[4] Xie H., Fujii M., Zhang X., Effect of Interfacial Nanolayer on the Effective Thermal Conductivity of Nanoparticle-Fluid Mixture, Int. J. Heat Mass Trans. 48 (2005) 2926–2932.

[5] Nguyen C.T., Desgranges F., Galanis N., Roy G., Maré T., Boucher S., Angue Mintsa H., Viscosity Data for Al2O3–Water Nanofluid-Hysteresis: Is Heat Transfer Enhancement Using Nanofluids Reliable?, Int. J. Therm. Sci. 47 (2008) 103–111.

[6] Masoumi N., Sohrabi N., Behzadmehr A., A New Model for Calculating the Effective Viscosity of Nanofluids, J. Phys. D: Appl. Phys. 42 (2009) 055501 (p. 6).

[7] Maige S.E., Nguyen C.T., Galanis N., Roy G., Heat Transfer Behaviors of Nano fluids in a Uniformly Heated Tube, Superlattices Microstruct. 35 (3-6) (2004) 543-557.

[8] Roy G., Nguyen C.T., Lajoie P.R., Numerical Investigation of Laminar Flow and Heat Transfer in a Radial Flow Cooling System with the Use of Nanofluids, Superlattices Microstruct. 35 (3-6) (2004) 497-511.

[9] Khanafer K., Vafai K., Lightstone M., Buoyancy Driven Heat Transfer Enhancement in a Two Dimensional Enclosure Utilizing Nanofluids, International Journal Heat Mass Transfer. 46 (2003) 3639-3653.

[10] Akbarinia A., Behzadmehr A., Numerical Study of Laminar Mixed Convection of a Nanofluid in Horizontal Curved Tubes, Journal Appl. Thermal Eng. 27 (2007) 1327-1337.

[11] Sundar L.S., Sharma K.V., Parveen S., Heat Transfer and Friction Factor Analysis in a Circular Tube with Al2O3 Nanofluid by Using Computational Fluid Dynamics, International Journal Nanoparticles. 2 (1-6) (2009) 191-199.

[12] Bianco V., Chiacchio F., Manca O., Nardini S., Numerical Investigation of Nanofluids Forced Convection in Circular Tubes, Appl. Thermal Eng. 29 (2009) 3632-3642.

[13] He Y., Men Y., Zhao Y., Lu H., Ding Y., Numerical Investigation into the Convective Heat Transfer of TiO2 Nanofluids Flowing Through a Straight Tube under the Laminar Flow Conditions, Appl. Thermal Eng. 29 (2009) 1965-1972.

[14] Abu-Nada E., Effects of Variable Viscosity and Thermal Conductivity of Al2O3– Water Nanofluid on Heat Transfer Enhancement in Natural Convection, International Journal Heat Fluid Flow. 30 (2009) 679-690.

[15] Abu-Nada E., Masoud Z., Hijazi A., Natural Convection Heat Transfer Enhancement in Horizontal Concentric Annuli Using Nanofluids, International Commun. Heat Mass Trans. 35(2008) 657-665.

[16] Izadi M., Behzadmehr A., Jalali-Vahida D., Numerical Study of Developing Laminar Forced Convection of a Nanofluid in an Annulus, International Journal Therm. Sci. 48 (2009) 2119-2129.

[17] Ben Mansour R., Galanis N., Nguyen C.T., Experimental Study of Mixed Convection with WatereAl2O3 Nanofluid in Inclined Tube with Uniform Wall Heat Flux, International Journal of Thermal Sciences. 50 (2011) 403-410.

[18] Mokhtari Moghari R., Akbarinia A., Shariat M., Talebi F., Laur R., Two Phase Mixed Convection Al2O3–Water Nanofluid Flow in an Annulus, International Journal of Multiphase Flow. 37 (2011) 585–595.

[19] Maxwell J.C., A Treatise on Electricity and Magnetism, second ed., Clarendon Press, Oxford University, UK, (1881).

[20] Pak B.C., Cho Y.I., Hydrodynamic and Heat Transfer Study of Dispersed Fluids with Submicron Metallic Oxide Particles, Exp. Heat Transfer. 11 (1998) 15.

[21] Xuan Y., Roetzel W., Conceptions for Heat Transfer Correlation of Nanofluids, International Journal Heat Mass Transfer. 43 (2000) 3701.

[22] Drew D.A., Passman S.L., Theory of Multi Component Fluids, Springer, Berlin, (1999).

[23] Khanafer K., Vafai K., Lightstone M., Buoyancy Driven Heat Transfer Enhancement in a Two Dimensional Enclosure Utilizing Nanofluids, International Journal Heat Mass Trans. 46 (2003) 3639–3653.